

# Boosting Adversarial Transferability with Spatial Adversarial Alignment

Zhaoyu Chen<sup>1\*</sup> Haijing Guo<sup>2,3\*</sup> Kaixun Jiang<sup>1</sup> Jiyuan Fu<sup>2</sup> Xinyu Zhou<sup>2</sup>  
 Dingkang Yang<sup>1</sup> Hao Tang<sup>4</sup> Bo Li<sup>5</sup> Wenqiang Zhang<sup>1,2†</sup>

<sup>1</sup>College of Intelligent Robotics and Advanced Manufacturing, Fudan University

<sup>2</sup>College of Computer Science and Artificial Intelligence, Fudan University

<sup>3</sup>China Southern Power Grid Artificial Intelligence Technology Co., Ltd.

<sup>4</sup>School of Computer Science, Peking University <sup>5</sup>vivo Mobile Communication Co., Ltd.

{zhaoyuchen20, wqzhang}@fudan.edu.cn, hjguo22@m.fudan.edu.cn

## Abstract

Deep neural networks are vulnerable to adversarial examples that exhibit transferability across various models. Numerous approaches are proposed to enhance the transferability of adversarial examples, including advanced optimization, data augmentation, and model modifications. However, these methods still show limited transferability, particularly in cross-architecture scenarios, such as from CNN to ViT. To achieve high transferability, we propose a technique termed Spatial Adversarial Alignment (SAA), which employs an alignment loss and leverages a witness model to fine-tune the surrogate model. Specifically, SAA consists of two key parts: spatial-aware alignment and adversarial-aware alignment. First, we minimize the divergences of features between the two models in both global and local regions, facilitating spatial alignment. Second, we introduce a self-adversarial strategy that leverages adversarial examples to impose further constraints, aligning features from an adversarial perspective. Through this alignment, the surrogate model is trained to concentrate on the common features extracted by the witness model. This facilitates adversarial attacks on these shared features, thereby yielding perturbations that exhibit enhanced transferability. Extensive experiments on various architectures on ImageNet show that aligned surrogate models based on SAA can provide higher transferable adversarial examples, especially in cross-architecture attacks.

## 1 Introduction

Deep neural networks (DNNs) have been successfully and extensively deployed across security-sensitive applications [32], including autonomous driving [63, 68, 67], facial verification [70, 69, 47, 9], and video surveillance [23, 72, 24, 20]. However, DNNs exhibit considerable vulnerability to adversarial examples [18, 39, 16, 6, 7, 5, 4, 30, 31, 33], where imperceptible perturbations are introduced into natural images, leading models to produce incorrect predictions. In real-world applications, DNNs are typically concealed from user access, necessitating adversaries to generate adversarial examples within a black-box setting, where no knowledge of the target model’s parameters or architecture is available. Adversarial transferability [13, 26, 51] plays a crucial role in black-box settings as it allows adversaries to effectively compromise target models by employing adversarial examples generated on surrogate models. In black-box settings, adversarial transferability plays a crucial role, which enables adversaries to leverage adversarial examples crafted on surrogate models

\*indicates equal contributions.

†indicates corresponding authors.

to effectively attack target models. Thus, generating highly transferable adversarial examples is instrumental in uncovering and understanding the vulnerabilities within DNNs, drawing substantial attention in recent research.

Cross-model transferability has been extensively studied for CNNs [13, 61, 14]. Highly transferable adversarial examples are usually based on advanced optimization [13, 29, 51] and data augmentation [61, 14, 37]. The principle is to alleviate the overfitting of adversarial examples on surrogate models, determining whether the attack can be successfully transferred to the target models. In addition, some model modification methods [59, 21], such as amplifying the gradient on skip connections (the structure in ResNet [22]), can also improve transferability. However, few works explore adversarial transferability on Vision Transformer (ViT) [15] and the performance of existing work extending CNN to ViT is poor due to significant structural differences. Specifically, ViT flattens the image into a sequence of patch tokens and employs multi-head self-attention to capture global relationships among the patches. In contrast, CNNs typically consist of stacked convolutional layers that learn feature relationships progressively through downsampling. Therefore, [58] first empirically analyzes the structure of ViT and propose PNA and PatchOut [58], but there is still much room for improvement in cross-architecture transferability.

In this paper, we argue that unique structural features are critical to cross-architecture adversarial transferability. Given a dataset, various models tend to exhibit analogous decision boundaries [34], arising from their ability to learn similar features. If we can obtain a surrogate model whose features are similar to those of models with different architectures, then the resulting adversarial perturbation can be transferable across different models. A recent technique known as Model Alignment (MA) [38] employs an alignment loss to minimize prediction divergences between surrogate models and witness models, thereby indirectly facilitating the extraction of features that are similarly represented by the witness model. However, directly applying MA to black-box attacks may lead to the degradation of cross-architecture transferability. The main reasons are: **(i)** Features are not aligned in space [58]. MA only uses the final prediction of the model, but in fact, the spatial features of ViT and CNN are different [71, 57]. It is difficult to directly constrain the similarity of features only by the final logits. **(ii)** Features are not aligned from the perspective of adversarial features. In addition to the features of clean images, the features of adversarial examples also have similarities across different models and need to be considered.

To overcome these challenges and enhance transferability, we propose a technique called Spatial Adversarial Alignment (SAA), which utilizes an alignment loss from the perspective of spatial and adversarial features and incorporates a witness model to refine the surrogate model. SAA consists of two key parts: spatial-aware alignment and adversarial-aware alignment. In the spatial-aware alignment, in addition to aligning on the final global features, we also focus on the features of local regions. We make local features of CNNs by position to align ViTs' embeddings at the same position. In the adversarial-aware alignment, we introduce a self-adversarial strategy, which constructs adversarial examples so that the model can learn the differences between different architectures in adversarial features, thereby enabling the model to further capture more common features. Aligned surrogate models by SAA provide promising adversarial transferability and can be seamlessly integrated with existing transfer attacks. In addition, we further summarize the empirical guidance for the selection of surrogate and witness models in SAA. Our contributions can be summarized as follows:

- We reveal for the first time the importance of spatial and adversarial features for cross-architecture transferability, which supports alignment with different models.
- We propose Spatial Adversarial Alignment (SAA), which leverages a witness model to fine-tune the surrogate model via spatial-aware and adversarial-aware alignment to generate highly transferable adversarial examples. In addition, we further summarize the empirical guidance for the model selection in SAA.
- Experiments on 6 CNNs and 4 ViTs show that SAA has state-of-the-art adversarial transferability, especially in cross-model transferability. Compared with MA, on ResNet50, the transferability from CNN to ViT is improved by 25.5-39.1%.

## 2 Methodology

### 2.1 Preliminaries

In this paper, we focus on the image classification task on DNNs. Let  $f_\theta(\cdot)$  represent a DNN-based classifier with different network parameters  $\theta$ . We denote the clean image as  $x$  and its corresponding ground-truth label as  $y$ . Following [13, 61, 14], we evaluate the adversarial transferability under untargeted adversarial attacks with  $l_\infty$  norm. Therefore, the goal of transfer attacks is to add an adversarial perturbation to the clean image  $x$  based on the information of the surrogate model  $f_{\theta_s}(\cdot)$  to obtain the adversarial example  $x_{adv}$  [18], so that  $f_{\theta_s}(x_{adv}) \neq y$  subject to the constraint that  $\|x_{adv} - x\|_\infty \leq \epsilon$ .

In the black-box setting, no information about the target model—such as its architecture, weights, or gradients—is accessible. Therefore, adversarial examples are generated solely by utilizing a surrogate model  $f_{\theta_s}(\cdot)$ , leveraging their transferability to deceive the target model  $f_{\theta_t}(\cdot)$ .

### 2.2 Spatial Adversarial Alignment (SAA)

Spatial Adversarial Alignment (SAA) employs an alignment loss tailored to both spatial and adversarial feature perspectives, incorporating a witness model to fine-tune the surrogate model. SAA aims to adjust the surrogate model to extract features closely aligned with those of the witness model, capturing both spatial and adversarial features shared across models. As shown in Figure 1, SAA consists of two parts, namely spatial-aware alignment and adversarial-aware alignment.

**Spatial-aware Alignment.** The purpose of spatial-aware alignment is to make the surrogate and witness models more consistent in the feature space. Naturally, the most intuitive approach to aligning the feature distributions of two models is to minimize the distance between their final outputs [38]. However, when the models exhibit significant architectural differences, ensuring output similarity alone is insufficient to achieve alignment in intermediate features. In black-box attacks, where the details of the target model’s architecture are unknown, this issue becomes more pronounced. Taking the challenging scenario of CNN to ViT as an example, their intermediate layer features differ substantially in semantic levels [71]. This discrepancy arises primarily from differences in receptive fields, stacking methodologies, and normalization techniques between CNNs and ViTs. Therefore, relying solely on output alignment for model fine-tuning indirectly captures some common features, but this approach can, in certain cases, result in degraded transferability, as observed in methods like Model Alignment (MA) [38].

Therefore, in addition to aligning on the final global features, we also need to focus on the features of local regions. For ease of understanding, we define the global features  $f_\theta(x)$  as the logits of the model corresponding to the input  $x$ . For CNNs, it is the output of features by the last layer. For ViTs, it refers to the final embedding of the [CLS] token after the MLP block. First, we perform alignment at the global feature level by defining an alignment loss between the surrogate model and witness model at the output layer:

$$\mathcal{L}_{global}(x; \theta_s) = D_{KL}(f_{\theta_s}(x), f_{\theta_w}(x)), \quad (1)$$

where  $D_{KL}$  measures the feature divergence with Kullback-Leibler (KL) divergence.

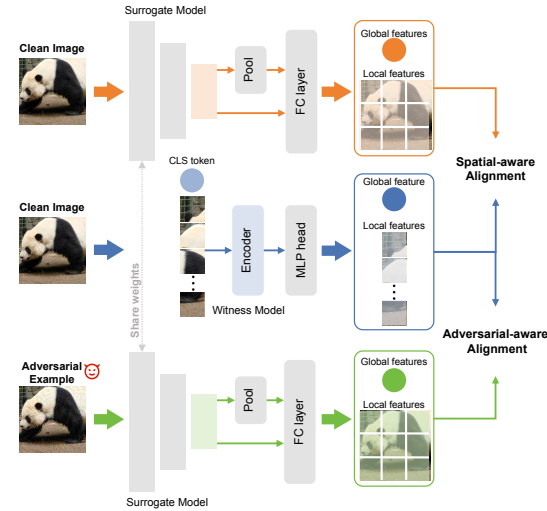


Figure 1: Spatial Adversarial Alignment (SAA) consists of two parts: spatial-aware alignment and adversarial-aware alignment. Initially, we aim to minimize the feature divergences between the two models across both global and local regions, thereby promoting spatial alignment. Subsequently, we introduce a self-adversarial strategy that utilizes adversarial examples to impose additional constraints, aligning the adversarial features.

Next, we align the models at the local feature level. Here, we define  $z_\theta(x)$  as local features. Each spatial position  $(h, w)$  within this feature map is treated as a distinct local region and the feature for each local region is  $z_\theta^{[q]}(x)$ , where  $q = \{1, 2, \dots, H \times W\}$ . Since every local feature is embedded with the corresponding sub-image and position information, regarding them as spatial dense predictions is reasonable. Let  $z_{\theta_s}^{[q]}(x)$  and  $z_{\theta_w}^{[q]}(x)$  denote the local features associated with each local region  $q$  for the surrogate model and witness model, respectively. For CNNs,  $z_\theta(x)^{B \times C \times H \times W}$  represents the logits generated by the final convolutional layer and then pass the final MLP. For ViTs,  $z_\theta(x)^{B \times C' \times H \times W}$ <sup>3</sup> is the embeddings of patch tokens after passing through the last MLP except for the [CLS] token, where each patch token corresponds to a specific spatial region in the input. Next, we argue pseudo-labels better aggregate local information, so we compute pseudo-labels of the local region  $q$  and denote this pseudo-label as  $\hat{y}_{\theta_w}^{[q]}$ , which is obtained by taking the arg max over the logits after the last MLP of the witness model:  $\hat{y}_{\theta_w}^{[q]} = \arg \max(z_{\theta_w}^{[q]}(x))$ . Then, we use this pseudo-label to supervise the learning of the local feature of the surrogate model. To achieve local alignment, we minimize the divergence of corresponding local regions' logits and the local alignment loss is expressed as:

$$\mathcal{L}_{local}(x; \theta_s) = \frac{1}{HW} \sum_{q=1}^{HW} D_{CE}(z_{\theta_s}^{[q]}(x), \hat{y}_{\theta_w}^{[q]}), \quad (2)$$

where  $D_{CE}$  is the cross-entropy loss. Therefore, the spatial-aware alignment loss is expressed as:

$$\mathcal{L}_{SA}(x; \theta_s) = \mathcal{L}_{global}(x; \theta_s) + \gamma \cdot \mathcal{L}_{local}(x; \theta_s), \quad (3)$$

where  $\gamma$  is the spatial factor. By minimizing this spatial-aware alignment loss, we encourage the surrogate model to produce features in both global and local regions that are consistent with those of the witness model, even across different architectures.

**Adversarial-aware Alignment.** The relationship between features and adversarial vulnerability is highly significant. Some hypotheses [64, 43] propose that adversarial examples possess distinct feature distributions compared to normal examples, which may inherently predispose models to adversarial vulnerability—a notion supported by several studies [1, 37]. Beyond normal examples, learning adversarial features may offer a way to capture shared features between surrogate models and witness models. Furthermore, [14] suggests that models trained with adversarial examples focus on more discriminative regions within images, displaying feature recognition patterns distinct from those of normally trained models. Thus, adversarial examples play a crucial role in achieving model alignment.

In our adversarial-aware alignment, we introduce a self-adversarial strategy that constructs adversarial examples of the surrogate model to enable the model to discern architectural differences in adversarial features effectively. Specifically, we leverage the gradients to iteratively generate adversarial examples under the supervision of the global features of the witness model. Assuming  $x_{adv}^{(0)} = x$ , we define the adversarial example  $x_{adv}^{(t+1)}$  of the surrogate model as:

$$x_{adv}^{(t+1)} = \Pi_{x, \epsilon} \left( x_{adv}^{(t)} + \alpha \cdot \text{sign} \left( \nabla_x D_{KL} \left( f_{\theta_s}(x_{adv}^{(t)}), f_{\theta_w}(x) \right) \right) \right), \quad (4)$$

where  $D_{KL}$  denotes the KL divergence,  $x_{adv}^{(t)}$  denotes the adversarial example at iteration  $t$ ,  $\alpha$  is the step size, and  $\Pi_\epsilon$  projects the adversarial example onto an  $\epsilon$ -bounded neighborhood around the original input  $x$ .

Once the adversarial example  $x_{adv}$  is generated, we also perform adversarial-aware alignment on the adversarial examples from global and local features to further align the surrogate and witness models. The loss of the adversarial-aware alignment is expressed as:

$$\mathcal{L}_{AA}(x_{adv}; \theta_s) = \mathcal{L}_{global}(x_{adv}; \theta_s) + \omega \cdot \mathcal{L}_{local}(x_{adv}; \theta_s), \quad (5)$$

where  $\omega$  is the adversarial factor.

**Optimization.** Combining spatial-aware and adversarial-aware alignment, the final optimization goal of spatial-adversarial alignment is:

$$\mathcal{L}_{SAA}(x; \theta_s) = \mathcal{L}_{SA}(x; \theta_s) + \kappa \cdot \mathcal{L}_{AA}(x_{adv}; \theta_s), \quad (6)$$

<sup>3</sup>Generally, ViT's patch embeddings  $z(x)$  is  $(B, N, C')$  by default. We first transform it to  $(B, C', H', W')$ , where  $N = H' \times W'$ . Then, we perform an adaptive pooling operation to transform it to  $(B, C', H, W)$ .

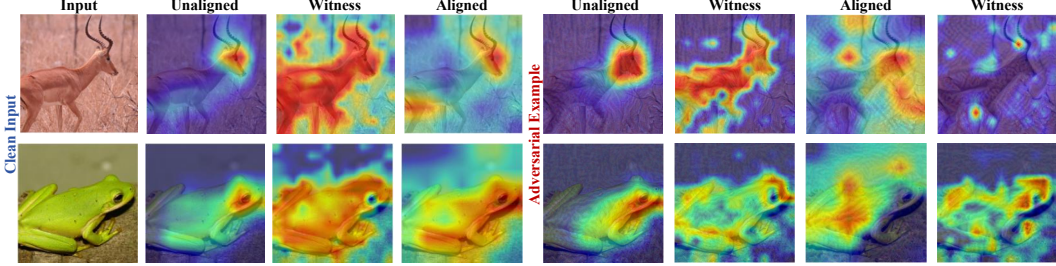


Figure 2: Grad-CAM visualizations comparing the feature distribution of unaligned and aligned surrogate models (Res50) on clean inputs and adversarial examples (generated by SSA-DI-TI-MI).

where  $\kappa$  is the alignment factor to balance the two alignments. If not otherwise stated, we define  $\gamma = 0.2$ ,  $\omega = 0.02$ , and  $\kappa = 0.02$  in this paper.

Spatial-adversarial alignment facilitates the alignment of the surrogate model with the witness model to further improve the adversarial transferability. The parameter update rule for the surrogate model, based on stochastic gradient descent (SGD), can be expressed as follows:

$$\theta_s^{(t+1)} = \theta_s^{(t)} - \eta \cdot \frac{1}{|\mathcal{B}|} \sum_{x \in \mathcal{B}} \nabla_{\theta_s^{(t)}} \mathcal{L}_{SAA}(x; \theta_s), \quad (7)$$

where  $t$  is the epoch,  $\eta$  is the learning rate and  $\mathcal{B}$  means the mini-batch samples. Please refer to **Algorithm 1** for the detailed loss calculation process.

### 2.3 A Close Look at SAA

To verify whether SAA significantly improves the spatial and adversarial features after model alignment, we conduct quantitative and qualitative analyses based on the models before and after alignment. We randomly sample 100 images from ImageNet val and then compute the cosine similarity between the global features of the surrogate models before and after applying SAA with different witness models. Table 1 shows that, whether for clean images or adversarial examples (generated by SSA-DI-TI-MI), the feature similarity improves after alignment. Notably, when the surrogate model is ViT-B, the improvement in similarity is even more pronounced. In addition, the feature gap between Res50 and Swin-B is indeed significant, but even so, SAA achieves a  $\frac{0.0551 - 0.0369}{0.0369} = 49.3\%$  improvement in similarity. This result suggests that, after applying SAA, the aligned surrogate models effectively capture features shared with the witness model, providing strong evidence of the alignment’s success.

Then, we use Grad-CAM [45]’s heatmaps to simulate the feature distribution of the model, as shown as Figure 2. For the **clean inputs** (first four cols), the heatmaps generated by the unaligned surrogate model (2-nd col) primarily focus on local regions of the object. In contrast, the aligned surrogate model (4-th col) heatmaps demonstrate more diffuse attention spread across the entire object, similar to that of the witness model (ViT-B, 3-rd col), which shows aligned surrogate models learn the common spatial features. For **adversarial examples** (last four cols), the 5-th and 7-th cols display the heatmaps of adversarial examples generated by the unaligned and aligned surrogate models, respectively. The 6-th and 8-th show the witness model’s responses to these adversarial examples. Notably, the adversarial examples generated by the unaligned surrogate model fail to effectively transfer to the witness model (6-th col) due to still focusing on the target subject, indicating limited cross-model transferability. In contrast, adversarial examples generated by the aligned surrogate model (7-th col) successfully transferred to the witness model (8-th col) as the features are spread out, demonstrating enhanced cross-model transferability achieved through SAA.

Table 1: Cosine similarity of global features of surrogate models.

Surrogate	Witness	Clean		Adv	
		Unaligned	Aligned	Unaligned	Aligned
Res50	Res50	<b>1.0000</b>	0.9949	<b>1.0000</b>	0.9922
	DN121	0.0573	<b>0.1153</b>	0.0700	<b>0.1328</b>
	ViT-B	0.0533	<b>0.1408</b>	0.0452	<b>0.1191</b>
	Swin-B	0.0352	<b>0.0448</b>	0.0369	<b>0.0551</b>
ViT-B	Res50	0.0566	<b>0.1323</b>	0.0672	<b>0.1544</b>
	DN121	0.4016	<b>0.6278</b>	0.4121	<b>0.6551</b>
	ViT-B	<b>1.0000</b>	0.9706	<b>1.0000</b>	0.9728
	Swin-B	0.3058	<b>0.5115</b>	0.3169	<b>0.4257</b>

### 3 Experiments

#### 3.1 Experimental Setup

**Datasets.** Our experiments utilize the ImageNet-compatible dataset [27], a widely adopted subset containing 1,000 images from the ImageNet validation set [11]. This dataset is commonly used in adversarial robustness studies, such as those in [61, 13, 14].

**Models.** To assess the adversarial transferability of different network architectures, we focus on convolutional neural networks (CNNs) and vision transformers (ViTs) as the target models. For CNNs, we select the typically trained ResNet-18 (Res18), ResNet-50 (Res50) and ResNet-101 (Res101) [22], VGG-19 [46], DenseNet-121 (DN121) [25], and Inception-v3 (Inc-v3) [48]. For ViTs, we evaluate the Vision Transformer (ViT-B) [15], Swin Transformer (Swin-B) [35], Pyramid Vision Transformer (PVT-v2) [52], and MobileViT-s (MobViT) [40].

**Metric.** Adversarial transferability is quantified by calculating the average attack success rate (Avg. ASR, %) across target models (excluding the surrogate model), with a higher success rate signifying enhanced transferability. In the paper, 'n/a' is the baseline and defined as the average attack success rate obtained by generating adversarial examples using the surrogate model without any alignment.

**Implementation Details.** In our experiments, we select the MI [13] attack as the baseline for generating adversarial examples with high transferability, as it is widely recognized within the field of adversarial transferability [14, 61, 53, 37, 54, 51, 29, 56, 59, 58]. For MI, we set the perturbation magnitude  $\epsilon = 16$  [13, 18], perform 10 iterations, with a step size of  $\frac{16}{10} = 1.6$ , and use a momentum  $\mu = 1$ . During the Spatial Adversarial Alignment, all surrogate models are fine-tuned for 1 epoch using stochastic gradient descent (SGD) with a momentum of 0.9, and no learning rate adjustments are applied. It is important to note that no additional data is used for fine-tuning, as it relies solely on the same training data used for both the surrogate and witness models. The number of adversarial examples generated by SAA is in a 1 : 1 ratio with the training dataset. The settings for Model Alignment (MA) [38] are consistent with the parameters specified in the original paper.

#### 3.2 Performance Comparison

**Performance comparison with alignment methods.** We first compare with existing alignment methods [38], where adversarial examples are generated based on MI [13]. Table 2 illustrates the performance difference between MA and SAA in terms of adversarial transferability, with SAA demonstrating a significant advantage over MA. For instance, when the surrogate model is Res50, and the witness model is also Res50, SAA achieves a 16.6% improvement in average ASR over the original surrogate model, compared to a modest 3.6% improvement with MA. This highlights that SAA, even without introducing additional information, enhances adversarial transferability through the alignment of adversarial features. Furthermore, when the witness models are DN121, ViT-B, and Swin-B, SAA outperforms MA by 11.9%, 10.4%, and 13.1%, respectively. In addition to the remarkable adversarial transferability that SAA provides, we make two other key observations: **(i)** MA only considers global features, which makes it difficult to align features between models with large differences, which may lead to a decrease in transferability. When the surrogate model is DN121 and the witness model is Swin-B, the ASR of ViT-B, Swin-B, PVT-v2, and MobViT is not as good as the origin DN121, which shows that relying solely on global features for alignment is not enough, and can only achieve poor transferability. **(ii)** SAA provides strong cross-architecture transferability. When the surrogate model is Res50, and the witness models are Res50, DN121, ViT-B, and Swin-B, the transferability of SAA on ViTs is improved by 39.06%, 31.29%, 25.51%, and 37.74% respectively compared with MA itself, and it also has high transferability between CNNs.

**Performance comparison with transfer attacks.** Aligned surrogate models by SAA have great potential for adversarial transferability, so existing transfer attacks such as advanced optimization and data augmentation can further improve transferability. Here, we choose Res50 as the surrogate model and ViT-B as the witness model, and superimpose them with MI [13], NI [29], GI [51], DI [61], TI [14] and SSA [37] to evaluate the transferability, as shown in Table 3. Taking GI and SSA as examples, the transferability of the model after SAA is improved by 21.7% and 8.4% respectively, compared with the origin surrogate model, which is a very significant improvement. When multiple attacks are integrated, such as SSA-DI-TI-MI, SAA further enhances the transferability by 2.0%, achieving an impressive 88.2% ASR, which closes white-box attacks' performance. This indicates

Table 2: Comparison of adversarial transferability on different alignment methods.

Surrogate	Witness	Attack	Target Model										Avg. ASR (%)	
			CNNs					ViTs						
			Res18	Res50	Res101	VGG19	DN121	Inc-v3	ViT-B	Swin-B	PVT-v2	MobViT		
Res50	n/a	MI	57.7	99.9	58.1	54.2	55.1	39.0	9.4	33.0	38.0	35.7	42.2	
		MA	60.4	99.8	56.4	60.3	67.3	44.3	12.1	35.6	37.2	39.0	45.8	
		SAA	<b>77.5</b>	<b>100.0</b>	<b>71.7</b>	<b>72.0</b>	<b>77.0</b>	<b>58.7</b>	<b>19.9</b>	<b>47.8</b>	<b>51.8</b>	<b>52.8</b>	<b>58.8</b>	
	DN121	MA	83.1	96.7	75.8	82.3	87.1	64.0	19.8	49.6	54.5	59.2	63.9	
		SAA	<b>92.4</b>	<b>98.6</b>	<b>87.1</b>	<b>90.3</b>	<b>94.6</b>	<b>77.8</b>	<b>30.5</b>	<b>64.2</b>	<b>69.2</b>	<b>76.5</b>	<b>75.8</b>	
		ViT-B	MA	74.2	99.2	63.5	69.3	72.8	51.5	18.5	41.5	42.7	47.4	53.5
	Swin-B	MA	<b>84.1</b>	<b>99.6</b>	<b>74.7</b>	<b>80.3</b>	<b>81.8</b>	<b>65.7</b>	<b>24.3</b>	<b>48.7</b>	<b>52.9</b>	<b>62.5</b>	<b>63.9</b>	
		SAA	<b>79.7</b>	<b>95.7</b>	<b>66.4</b>	<b>74.1</b>	<b>75.9</b>	<b>56.9</b>	<b>19.6</b>	<b>41.9</b>	<b>47.9</b>	<b>55.2</b>	<b>57.5</b>	
		n/a	MI	84.4	69.6	54.8	76.6	100.0	56.5	16.2	42.1	43.9	52.6	58.6
DN121	n/a	MA	88.8	65.8	49.8	78.3	<b>100.0</b>	55.7	14.9	40.0	38.2	53.0	57.6	
		SAA	<b>95.7</b>	<b>80.3</b>	<b>70.9</b>	<b>87.7</b>	99.6	<b>78.2</b>	<b>31.4</b>	<b>55.0</b>	<b>56.6</b>	<b>72.1</b>	<b>71.9</b>	
		DN121	MA	79.3	69.5	54.9	78.8	<b>100.0</b>	55.4	12.3	39.9	41.7	52.4	57.2
	DN121	SAA	<b>90.1</b>	<b>81.4</b>	<b>71.5</b>	<b>87.9</b>	99.9	<b>75.0</b>	<b>25.3</b>	<b>54.9</b>	<b>56.4</b>	<b>69.7</b>	<b>70.1</b>	
		ViT-B	MA	89.6	80.6	71.1	88.1	<b>100.0</b>	70.0	22.4	53.9	58.4	68.7	69.1
		SAA	<b>94.0</b>	<b>83.6</b>	<b>75.2</b>	<b>90.3</b>	99.8	<b>81.7</b>	<b>27.2</b>	<b>58.0</b>	<b>59.1</b>	<b>80.3</b>	<b>74.0</b>	
	Swin-B	MA	88.3	63.9	49.2	77.8	<b>100.0</b>	54.4	14.5	38.1	37.5	52.2	56.9	
		SAA	<b>94.8</b>	<b>80.0</b>	<b>69.1</b>	<b>88.0</b>	99.7	<b>74.4</b>	<b>26.3</b>	<b>50.2</b>	<b>51.6</b>	<b>71.2</b>	<b>69.5</b>	
		n/a	MI	48.6	41.0	31.9	58.1	50.8	44.4	100.0	58.1	44.7	47.4	53.8
ViT-B	n/a	MA	65.8	51.9	43.0	66.9	60.0	51.5	99.7	66.0	57.3	57.6	63.1	
		SAA	<b>87.3</b>	<b>80.6</b>	<b>75.9</b>	<b>86.1</b>	<b>87.5</b>	<b>78.0</b>	<b>99.9</b>	<b>91.0</b>	<b>85.4</b>	<b>85.2</b>	<b>86.3</b>	
		DN121	MA	88.9	73.6	67.6	89.1	87.8	74.9	<b>100.0</b>	84.9	78.3	82.7	83.8
	DN121	SAA	<b>94.7</b>	<b>86.8</b>	<b>81.3</b>	<b>93.8</b>	<b>94.0</b>	<b>86.6</b>	99.8	<b>91.3</b>	<b>87.2</b>	<b>90.7</b>	<b>91.0</b>	
		ViT-B	MA	54.3	37.2	29.2	56.0	47.9	42.4	<b>100.0</b>	52.8	42.3	47.4	52.5
		SAA	<b>62.7</b>	<b>46.9</b>	<b>40.9</b>	<b>64.2</b>	<b>57.5</b>	<b>52.1</b>	100.0	<b>59.5</b>	<b>52.6</b>	<b>58.8</b>	<b>60.9</b>	
	Swin-B	MA	66.6	46.0	38.3	67.5	57.6	50.8	<b>99.7</b>	65.7	53.6	58.2	62.0	
		SAA	<b>83.0</b>	<b>69.2</b>	<b>65.6</b>	<b>81.2</b>	<b>78.1</b>	<b>74.2</b>	99.3	<b>84.3</b>	<b>76.0</b>	<b>78.3</b>	<b>80.0</b>	
		n/a	MI	48.2	31.3	20.0	49.3	34.3	29.7	13.9	100.0	45.4	41.4	42.5
Swin-B	n/a	MA	54.8	50.9	36.5	61.8	49.3	40.1	32.4	<b>100.0</b>	68.5	55.6	55.4	
		SAA	<b>90.3</b>	<b>85.3</b>	<b>77.9</b>	<b>92.0</b>	<b>88.4</b>	<b>76.4</b>	<b>64.7</b>	99.9	<b>92.4</b>	<b>89.0</b>	<b>85.7</b>	
		DN121	MA	77.3	71.4	60.0	83.9	76.4	60.7	49.0	<b>100.0</b>	85.9	80.9	74.9
	DN121	SAA	<b>94.9</b>	<b>91.7</b>	<b>85.8</b>	<b>96.5</b>	<b>94.7</b>	<b>85.6</b>	<b>74.3</b>	<b>100.0</b>	<b>95.5</b>	<b>95.4</b>	<b>91.4</b>	
		ViT-B	MA	62.6	52.8	40.0	66.2	55.3	45.6	34.0	<b>100.0</b>	70.1	61.8	59.5
		SAA	<b>84.7</b>	<b>80.0</b>	<b>74.2</b>	<b>90.5</b>	<b>85.5</b>	<b>75.7</b>	<b>70.3</b>	<b>100.0</b>	<b>91.9</b>	<b>88.6</b>	<b>84.6</b>	
	Swin-B	MA	62.6	52.8	40.0	66.2	55.3	45.6	<b>34.0</b>	<b>100.0</b>	70.1	61.8	59.5	
		SAA	<b>73.5</b>	<b>58.9</b>	<b>45.7</b>	<b>79.2</b>	<b>63.4</b>	<b>50.7</b>	32.8	<b>100.0</b>	<b>75.8</b>	<b>71.4</b>	<b>65.8</b>	

that SAA substantially narrows the performance gap between black-box and white-box attacks, thereby facilitating a more comprehensive evaluation of the adversarial robustness of existing models.

**Performance comparison with attacks on ViTs.** To further explore the cross-architecture transferability, we evaluate adversarial attacks on ViTs, including SGM [59], PatchOut [58], PNA [58], and TGR [66]. Here, we choose the surrogate model as ViT-B and the witness model as Res50. In PatchOut, SAA first improves the transferability between ViTs, for example, the ASR from ViT-B to Swin-B is improved by 42.6%. Secondly, SAA greatly improves the transferability from ViT to CNNs, for example, the ASR is improved by 45.0% and 42.0% on Res50 and DN121 respectively. On SGM, PNA, and TGR, SAA also achieves stronger cross-architecture transferability without modifying the forward and backward propagation of the model.

**Summary.** Although we conduct 16 combinations and evaluate on 6 CNNs and 4 ViTs, showing that SAA’s improvement is not limited to specific choices of witness models. Based on the above experiments, we further summarize the empirical guidance for the selection of surrogate and witness models: **i)** Self-alignment (surrogate and witness models are consistent) usually only provides minor improvements (it is difficult to learn unique structural features), and alignment between different models improves more significantly. **ii)** When the surrogate model is a ViT-like model and the witness model is a CNN-like model, better cross-architecture transferability can be obtained. This is mainly because ViT has stronger performance, while CNN further provides unique structural features. It should be noted that the target models are unknown in the transfer attack, so no information of the target models can be used for alignment.

Table 3: SAA has stronger adversarial transferability with existing transfer attacks.

Attack	Target Model										Avg. ASR (%)	
	CNNs						ViTs					
	Res18	Res50	Res101	VGG19	DN121	Inc-v3	ViT-B	Swin-B	PVT-v2	MobViT		
MI	57.7	<b>99.9</b>	58.1	54.2	55.1	39.0	9.4	33.0	38.0	35.7	42.2	
MI-SAA	<b>84.1</b>	99.6	<b>74.7</b>	<b>80.3</b>	<b>81.8</b>	<b>65.7</b>	<b>24.3</b>	<b>48.7</b>	<b>52.9</b>	<b>62.5</b>	<b>63.9</b>	
NI	58.9	<b>100.0</b>	63.2	59.3	61.4	40.0	9.6	37.4	41.8	38.1	45.5	
NI-SAA	<b>86.1</b>	<b>99.9</b>	<b>76.3</b>	<b>82.2</b>	<b>83.7</b>	<b>67.6</b>	<b>24.0</b>	<b>50.6</b>	<b>55.7</b>	<b>64.8</b>	<b>65.7</b>	
GI	57.3	<b>100.0</b>	62.3	60.5	60.5	40.7	12.5	36.8	40.7	39.6	45.7	
GI-SAA	<b>86.5</b>	99.7	<b>78.8</b>	<b>83.9</b>	<b>84.8</b>	<b>70.4</b>	<b>27.6</b>	<b>52.7</b>	<b>55.8</b>	<b>66.3</b>	<b>67.4</b>	
DI	44.1	<b>95.8</b>	41.7	56.1	44.2	26.1	5.6	30.9	36.7	35.1	35.6	
DI-SAA	<b>74.6</b>	94.4	<b>61.1</b>	<b>81.1</b>	<b>73.2</b>	<b>53.1</b>	<b>10.6</b>	<b>44.0</b>	<b>50.8</b>	<b>63.6</b>	<b>56.9</b>	
TI	38.5	<b>99.9</b>	<b>37.8</b>	33.9	36.1	24.2	5.4	21.0	29.0	21.1	27.4	
TI-SAA	<b>59.7</b>	94.9	35.2	<b>50.6</b>	<b>54.5</b>	<b>40.6</b>	<b>9.5</b>	<b>22.8</b>	<b>29.3</b>	<b>33.6</b>	<b>37.3</b>	
SSA	75.8	<b>99.9</b>	<b>78.6</b>	76.0	77.8	57.0	16.5	<b>48.5</b>	55.0	50.5	59.5	
SSA-SAA	<b>91.5</b>	99.5	77.8	<b>85.7</b>	<b>88.4</b>	<b>74.9</b>	<b>23.4</b>	46.7	<b>57.1</b>	<b>66.0</b>	<b>67.9</b>	
DI-MI	65.5	97.0	65.0	74.7	65.7	49.1	16.4	49.0	54.9	57.9	55.4	
DI-MI-SAA	<b>91.9</b>	<b>98.7</b>	<b>84.9</b>	<b>94.1</b>	<b>90.5</b>	<b>78.3</b>	<b>34.1</b>	<b>69.8</b>	<b>76.1</b>	<b>86.8</b>	<b>78.5</b>	
TI-MI	61.4	<b>99.9</b>	60.5	60.9	60.9	44.3	15.2	37.4	42.3	41.8	47.2	
TI-MI-SAA	<b>84.8</b>	99.3	<b>71.9</b>	<b>79.0</b>	<b>81.8</b>	<b>69.1</b>	<b>27.0</b>	<b>45.0</b>	<b>52.8</b>	<b>62.4</b>	<b>63.8</b>	
SSA-MI	89.6	<b>99.9</b>	92.2	89.5	91.0	77.6	39.2	<b>74.4</b>	76.4	76.3	78.5	
SSA-MI-SAA	<b>96.3</b>	99.8	<b>95.6</b>	<b>96.5</b>	<b>97.2</b>	<b>91.5</b>	<b>46.3</b>	74.1	<b>80.4</b>	<b>88.4</b>	<b>85.1</b>	
SSA-DI-TI-MI	93.5	98.5	92.3	95.0	93.7	85.5	<b>55.9</b>	<b>83.2</b>	87.1	89.8	86.2	
SSA-DI-TI-MI-SAA	<b>97.5</b>	<b>98.8</b>	<b>93.8</b>	<b>97.6</b>	<b>96.7</b>	<b>94.3</b>	53.6	81.6	<b>84.4</b>	<b>94.7</b>	<b>88.2</b>	

Table 4: SAA further improves the adversarial transferability of adversarial attacks on ViTs.

Attack	Target Model										Avg. ASR (%)	
	CNNs						ViTs					
	Res18	Res50	Res101	VGG19	DN121	Inc-v3	ViT-B	Swin-B	PVT-v2	MobViT		
SGM	82.9	67.6	59.4	81.2	75.4	71.3	<b>99.7</b>	83.3	72.7	78.8	78.3	
SGM-SAA	<b>91.1</b>	<b>79.8</b>	<b>73.3</b>	<b>87.5</b>	<b>87.3</b>	<b>80.9</b>	99.5	<b>90.5</b>	<b>82.6</b>	<b>86.3</b>	<b>86.6</b>	
PatchOut	45.6	27.4	20.3	45.5	36.1	33.9	93.0	41.0	34.2	40.5	43.3	
PatchOut-SAA	<b>76.5</b>	<b>72.4</b>	<b>70.3</b>	<b>79.4</b>	<b>78.1</b>	<b>71.3</b>	<b>94.7</b>	<b>83.6</b>	<b>77.2</b>	<b>76.8</b>	<b>78.7</b>	
PNA	61.2	45.0	38.1	60.8	54.8	49.0	<b>99.6</b>	66.3	55.8	56.8	60.3	
PNA-SAA	<b>82.7</b>	<b>78.1</b>	<b>73.4</b>	<b>85.6</b>	<b>84.0</b>	<b>75.1</b>	97.4	<b>89.3</b>	<b>80.3</b>	<b>82.1</b>	<b>83.3</b>	
TGR	74.0	55.6	48.4	73.2	66.6	59.0	<b>99.3</b>	74.5	61.6	69.6	69.6	
TGR-SAA	<b>85.9</b>	<b>78.1</b>	<b>71.5</b>	<b>87.4</b>	<b>85.6</b>	<b>79.6</b>	<b>99.3</b>	<b>89.1</b>	<b>81.0</b>	<b>86.2</b>	<b>85.1</b>	

### 3.3 Ensemble Attacks

The ensemble of multiple surrogate models can further improve adversarial transferability [13], so we want to explore whether SAA can further improve transferability. In the setting of ensemble attacks, we follow the setting of MI [13] and use the logits of multiple surrogate models for integration. Here we choose multiple groups of settings, such as Res50 (ViT-B) means that the surrogate model is Res50 and the witness model is ViT-B. Res50+ViT-B means the logits of these two models are integrated, and so on. As shown in Table 5, SAA further improves the performance of ensemble attacks. First, the alignment-based method is not as good as the direct integration strategy in white-box performance, but it has significant improvement in black-box transferability. For example, on (Res50+ViT-B), MA and SAA are 9.1% and 20.8% higher than the direct ensemble ASR, respectively. Then, MA directly constrains global features and does not take into account the huge differences in features between different structures, which may lead to degradation of transferability, such as on Swin-B. Finally, SAA has achieved state-of-the-art transferability and further enhance ensemble attacks because it considers spatial and adversarial features from a structural perspective.

### 3.4 Adversarial Defenses

To illustrate the effect of SAA in the face of adversarial defenses, we choose Inc-v3<sub>ens3</sub> as the target model and evaluate its performance on 12 adversarial defenses, including HGD [28], R&P [60],

Table 5: SAA improves the adversarial transferability of ensemble attacks.

Surrogate	Attack	Target Model										Avg. ASR (%)	
		CNNs					ViTs						
		Res18	Res50	Res101	VGG19	DN121	Inc-v3	ViT-B	Swin-B	PVT-v2	MobViT		
Res50	n/a	57.7	99.9	58.1	54.2	55.1	39.0	9.4	33.0	38.0	35.7	42.2	
ViT-B	n/a	48.6	41.0	31.9	58.1	50.8	44.4	100.0	58.1	44.7	47.4	47.2	
Res50+ViT-B	n/a	61.3	<b>100.0</b>	63.0	60.8	61.2	45.0	<b>97.6</b>	50.4	51.3	48.1	55.1	
Res50(Res50)+Res50(ViT-B)	MA	79.3	<b>100.0</b>	74.5	72.3	80.0	56.3	20.3	47.4	51.7	52.3	64.2	
	SAA	<b>86.8</b>	<b>100.0</b>	<b>85.9</b>	<b>83.9</b>	<b>86.7</b>	<b>70.0</b>	30.7	<b>60.4</b>	<b>64.1</b>	<b>69.6</b>	<b>75.9</b>	
Res50+DN121+ViT-B+Swin-B	n/a	65.4	<b>100.0</b>	78.0	79.1	<b>99.8</b>	62.0	<b>93.3</b>	<b>100.0</b>	77.4	68.9	71.8	
Res50(Res50)+Res50(DN121)+Res50(ViT-B)+Res50(Swin-B)	MA	87.0	99.8	85.4	83.2	90.0	67.2	28.0	60.3	66.2	63.9	75.5	
Res50(ViT-B)+Res50(Swin-B)	SAA	<b>93.5</b>	<b>100.0</b>	<b>92.9</b>	<b>92.1</b>	95.1	<b>82.3</b>	39.6	71.8	<b>80.4</b>	<b>81.7</b>	<b>87.2</b>	

Table 6: SAA improves adversarial transferability against adversarial defenses.

Attack	HGD	R&P	NIPS-r3	JPEG	FD	RS	Bit-Red	NRP	Diffpure	Inc-v3 <sub>ens3</sub>	Inc-v3 <sub>ens4</sub>	IncRes-v2 <sub>ens</sub>	Avg. ASR (%)
MI	42.5	21.9	25.3	33.9	42.4	23.6	29.3	6.7	13.8	33.3	31.3	23.3	27.3
MI-SAA	<b>73.3</b>	<b>57.8</b>	<b>60.4</b>	<b>69.9</b>	<b>65.6</b>	<b>39.6</b>	<b>42.3</b>	<b>12.0</b>	<b>22.4</b>	<b>68.9</b>	<b>65.5</b>	<b>57.9</b>	<b>53.0</b>
SSA-DI-TI-MI	93.7	89.6	90.2	91.9	89.7	82.3	81.7	14.8	71.1	92.5	91.1	89.8	81.5
SSA-DI-TI-MI-SAA	<b>96.0</b>	<b>93.2</b>	<b>94.8</b>	<b>95.1</b>	<b>94.0</b>	<b>89.8</b>	<b>85.5</b>	<b>20.2</b>	<b>78.8</b>	<b>95.7</b>	<b>94.5</b>	<b>93.3</b>	<b>85.9</b>

Table 7: Ablation study on alignment modules.

Module	Target Model										Avg. ASR (%)	
	Spatial	Adversarial	CNNs					ViTs				
			Res18	Res50	Res101	VGG19	DN121	Inc-v3	ViT-B	Swin-B	PVT-v2	MobViT
			57.7	<b>99.9</b>	58.1	54.2	55.1	39.0	9.4	33.0	38.0	35.7
✓			60.4	99.8	56.4	60.3	67.3	44.3	12.1	35.6	37.2	39.0
✓	✓		67.5	98.0	58.1	69.1	70.1	49.9	12.2	37.7	38.9	47.7
✓		✓	81.6	97.9	68.1	53.0	79.8	63.6	<b>25.5</b>	47.9	48.7	57.3
✓	✓	✓	<b>84.1</b>	99.6	<b>74.7</b>	<b>80.3</b>	<b>81.8</b>	<b>65.7</b>	24.3	<b>48.7</b>	<b>52.9</b>	<b>62.5</b>
												<b>63.9</b>

NIPS-r3<sup>4</sup>, JPEG [19], FD [36], RS [10], Bit-Red [62], NRP [41], Diffpure [43], Inc-v3<sub>ens3</sub> [50], Inc-v3<sub>ens4</sub> [50], and IncRes-v2<sub>ens</sub> [50]. Here we use the ensemble attack setting, and the surrogate models are Res50(Res50)+Res50(DN121)+Res50(ViT-B)+Res50(Swin-B). As shown in Table 6, although adversarial defenses weaken transferability, SAA still achieves a significant improvement in adversarial transferability compared to the origin surrogate models.

### 3.5 Ablation Studies

We select ResNet-50 as the surrogate model and ViT-B as the witness model for ablation studies (see **Appendix C** for more details, including training epochs, distance metric, GPU memory and computing cost, self-adversarial strategy).

**Alignment Module.** In spatial-aware alignment, ‘global’ represents  $\mathcal{L}_{global}$  (Equation 1), while ‘local’ represents  $\mathcal{L}_{local}$  (Equation 2). Similarly, ‘adversarial’ represents  $\mathcal{L}_{AA}$  (Equation 5) of adversarial-aware alignment. As shown in Table 7, when global features are introduced into the alignment, the transferability of the aligned surrogate model will increase by 3.6%. Based on  $\mathcal{L}_{global}$ , when only local features are introduced, the overall transferability is improved by 4.3% due to better alignment of features of different architectures in local regions, especially by 8.7% on MobViT. Since intermediate layer features between models are diverse and different, we choose last layer features that summarize the spatial information, which is a simple and effective strategy. Based on  $\mathcal{L}_{global}$ , when only adversarial features are introduced, the transferability is greatly improved, reaching 12.6% ASR, and the improvement is significant on ViTs. Finally, by integrating all features, the aligned surrogate model achieves state-of-the-art transferability.

## 4 Conclusions

In this study, we introduce a novel technique called Spatial Adversarial Alignment (SAA), which incorporates an alignment loss function and utilizes a witness model to fine-tune a surrogate model by focusing on both spatial-aware and adversarial-aware alignments. Through experimental analysis, we

<sup>4</sup><https://github.com/anlthms/nips-2017/tree/master/mmd>

show that leveraging these spatial and adversarial features for model alignment significantly enhances the adversarial transferability of surrogate models, with a particularly pronounced improvement in their cross-architecture capabilities. SAA not only integrates seamlessly with existing transfer attack strategies but also further amplifies adversarial transferability, thereby contributing to a more complete evaluation of the adversarial robustness of DNNs.

**Boarder Impacts.** Adversarial examples by SAA exhibit enhanced adversarial transferability, especially in cross-architecture capabilities. This poses a huge threat to the deployment of real-world applications. Simultaneously, it is also conducive to better evaluating their adversarial robustness.

**Limitations.** The huge gaps between network architectures limit transferability. While SAA aligns unique features under both spatial and adversarial conditions to mitigate these gaps, it does not fully resolve them. Then, SAA also introduces some computing costs during the alignment but no extra costs during attacking. In addition, a theoretical analysis is lacking. We have made significant progress, but there is still much to be done in addressing this issue.

**Acknowledgments.** This work was supported by National Natural Science Foundation of China (No.62576109, 62072112).

## References

- [1] Junyoung Byun, Myung-Joon Kwon, Seungju Cho, Yoonji Kim, and Changick Kim. Introducing competition to boost the transferability of targeted adversarial examples through clean feature mixup. In *IEEE/CVF Conference on Computer Vision and Pattern Recognition, CVPR 2023, Vancouver, BC, Canada, June 17-24, 2023*, pages 24648–24657. IEEE, 2023.
- [2] Yanbei Chen, Yongqin Xian, A. Sophia Koepke, Ying Shan, and Zeynep Akata. Distilling audio-visual knowledge by compositional contrastive learning. In *IEEE Conference on Computer Vision and Pattern Recognition, CVPR 2021, virtual, June 19-25, 2021*, pages 7016–7025. Computer Vision Foundation / IEEE, 2021.
- [3] Zhaoyu Chen, Bo Li, Kaixun Jiang, Shuang Wu, Shouhong Ding, and Wenqiang Zhang. Exploring decision-based black-box attacks on face forgery detection. *arXiv preprint arXiv:2310.12017*, 2023.
- [4] Zhaoyu Chen, Bo Li, Shuang Wu, Shouhong Ding, and Wenqiang Zhang. Query-efficient decision-based black-box patch attack. *IEEE Transactions on Information Forensics and Security*, 18:5522–5536, 2023.
- [5] Zhaoyu Chen, Bo Li, Shuang Wu, Kaixun Jiang, Shouhong Ding, and Wenqiang Zhang. Content-based unrestricted adversarial attack. In *Advances in Neural Information Processing Systems*, volume 36, pages 51719–51733, 2023.
- [6] Zhaoyu Chen, Bo Li, Shuang Wu, Jianghe Xu, Shouhong Ding, and Wenqiang Zhang. Shape matters: deformable patch attack. In *European Conference on Computer Vision*, pages 529–548. Springer, 2022.
- [7] Zhaoyu Chen, Bo Li, Jianghe Xu, Shuang Wu, Shouhong Ding, and Wenqiang Zhang. Towards practical certifiable patch defense with vision transformer. In *Proceedings of the IEEE/CVF Conference on Computer Vision and Pattern Recognition*, pages 15148–15158, 2022.
- [8] Zhengsu Chen, Lingxi Xie, Jianwei Niu, Xuefeng Liu, Longhui Wei, and Qi Tian. Visformer: The vision-friendly transformer. In *2021 IEEE/CVF International Conference on Computer Vision, ICCV 2021, Montreal, QC, Canada, October 10-17, 2021*, pages 569–578. IEEE, 2021.
- [9] Hai Ci, Pei Yang, Yiren Song, and Mike Zheng Shou. Ringid: Rethinking tree-ring watermarking for enhanced multi-key identification. In *European Conference on Computer Vision*, pages 338–354. Springer, 2024.
- [10] Jeremy M. Cohen, Elan Rosenfeld, and J. Zico Kolter. Certified adversarial robustness via randomized smoothing. In Kamalika Chaudhuri and Ruslan Salakhutdinov, editors, *Proceedings of the 36th International Conference on Machine Learning, ICML 2019, 9-15 June 2019, Long Beach, California, USA*, volume 97 of *Proceedings of Machine Learning Research*, pages 1310–1320. PMLR, 2019.
- [11] Jia Deng, Wei Dong, Richard Socher, Li-Jia Li, Kai Li, and Fei-Fei Li. Imagenet: A large-scale hierarchical image database. In *CVPR*, pages 248–255, 2009.
- [12] Terrance DeVries. Improved regularization of convolutional neural networks with cutout. *arXiv preprint arXiv:1708.04552*, 2017.
- [13] Yinpeng Dong, Fangzhou Liao, Tianyu Pang, Hang Su, Jun Zhu, Xiaolin Hu, and Jianguo Li. Boosting adversarial attacks with momentum. In *2018 IEEE Conference on Computer Vision and Pattern Recognition, CVPR 2018, Salt Lake City, UT, USA, June 18-22, 2018*, pages 9185–9193. Computer Vision Foundation / IEEE Computer Society, 2018.
- [14] Yinpeng Dong, Tianyu Pang, Hang Su, and Jun Zhu. Evading defenses to transferable adversarial examples by translation-invariant attacks. In *Proceedings of the IEEE/CVF Conference on Computer Vision and Pattern Recognition*, pages 4312–4321, 2019.
- [15] Alexey Dosovitskiy, Lucas Beyer, Alexander Kolesnikov, Dirk Weissenborn, Xiaohua Zhai, Thomas Unterthiner, Mostafa Dehghani, Matthias Minderer, Georg Heigold, Sylvain Gelly, Jakob Uszkoreit, and Neil Houlsby. An image is worth 16x16 words: Transformers for image recognition at scale. In *ICLR*, 2021.
- [16] F. Croce and M. Hein. Reliable evaluation of adversarial robustness with an ensemble of diverse parameter-free attacks. volume 119, pages 2206–2216, 2020.
- [17] Aditya Ganeshan, Vivek BS, and R Venkatesh Babu. Fda: Feature disruptive attack. In *Proceedings of the IEEE/CVF International Conference on Computer Vision*, pages 8069–8079, 2019.

[18] Ian J. Goodfellow, Jonathon Shlens, and Christian Szegedy. Explaining and harnessing adversarial examples. In *ICLR*, 2015.

[19] Chuan Guo, Mayank Rana, Moustapha Cisse, and Laurens Van Der Maaten. Countering adversarial images using input transformations. *arXiv preprint arXiv:1711.00117*, 2017.

[20] Pinxue Guo, Wanyun Li, Hao Huang, Lingyi Hong, Xinyu Zhou, Zhaoyu Chen, Jinglun Li, Kaixun Jiang, Wei Zhang, and Wenqiang Zhang. X-prompt: Multi-modal visual prompt for video object segmentation. In *Proceedings of the 32nd ACM International Conference on Multimedia*, pages 5151–5160, 2024.

[21] Yiwen Guo, Qizhang Li, and Hao Chen. Backpropagating linearly improves transferability of adversarial examples. In *Advances in Neural Information Processing Systems 33: Annual Conference on Neural Information Processing Systems 2020, NeurIPS 2020, December 6-12, 2020, virtual*, 2020.

[22] Kaiming He, Xiangyu Zhang, Shaoqing Ren, and Jian Sun. Deep residual learning for image recognition. In *CVPR*, pages 770–778, 2016.

[23] Lingyi Hong, Wenchao Chen, Zhongying Liu, Wei Zhang, Pinxue Guo, Zhaoyu Chen, and Wenqiang Zhang. Lvos: A benchmark for long-term video object segmentation. In *Proceedings of the IEEE/CVF International Conference on Computer Vision*, pages 13480–13492, 2023.

[24] Lingyi Hong, Shilin Yan, Renrui Zhang, Wanyun Li, Xinyu Zhou, Pinxue Guo, Kaixun Jiang, Yiting Chen, Jinglun Li, Zhaoyu Chen, et al. Onetracker: Unifying visual object tracking with foundation models and efficient tuning. In *Proceedings of the IEEE/CVF Conference on Computer Vision and Pattern Recognition*, pages 19079–19091, 2024.

[25] Gao Huang, Zhuang Liu, Laurens van der Maaten, and Kilian Q. Weinberger. Densely connected convolutional networks. In *CVPR*, pages 2261–2269, 2017.

[26] Kaixun Jiang, Lingyi Hong, Zhaoyu Chen, Pinxue Guo, Zeng Tao, Yan Wang, and Wenqiang Zhang. Exploring the adversarial robustness of video object segmentation via one-shot adversarial attacks. In *Proceedings of the 31st ACM International Conference on Multimedia*, pages 8598–8607, 2023.

[27] Alexey Kurakin, Ian J Goodfellow, and Samy Bengio. Adversarial examples in the physical world. In *Artificial intelligence safety and security*, pages 99–112. Chapman and Hall/CRC, 2018.

[28] Fangzhou Liao, Ming Liang, Yinpeng Dong, Tianyu Pang, Xiaolin Hu, and Jun Zhu. Defense against adversarial attacks using high-level representation guided denoiser. In *2018 IEEE Conference on Computer Vision and Pattern Recognition, CVPR 2018, Salt Lake City, UT, USA, June 18-22, 2018*, pages 1778–1787. Computer Vision Foundation / IEEE Computer Society, 2018.

[29] Jiadong Lin, Chuabiao Song, Kun He, Liwei Wang, and John E. Hopcroft. Nesterov accelerated gradient and scale invariance for adversarial attacks. In *8th International Conference on Learning Representations, ICLR 2020, Addis Ababa, Ethiopia, April 26-30, 2020*. OpenReview.net, 2020.

[30] Daizong Liu and Wei Hu. Imperceptible transfer attack and defense on 3d point cloud classification. *IEEE transactions on pattern analysis and machine intelligence*, 45(4):4727–4746, 2022.

[31] Daizong Liu, Wei Hu, and Xin Li. Point cloud attacks in graph spectral domain: When 3d geometry meets graph signal processing. *IEEE Transactions on Pattern Analysis and Machine Intelligence*, 2023.

[32] Daizong Liu, Mingyu Yang, Xiaoye Qu, Pan Zhou, Yu Cheng, and Wei Hu. A survey of attacks on large vision-language models: Resources, advances, and future trends. *arXiv preprint arXiv:2407.07403*, 2024.

[33] Siao Liu, Zhaoyu Chen, Wei Li, Jiwei Zhu, Jiafeng Wang, Wenqiang Zhang, and Zhongxue Gan. Efficient universal shuffle attack for visual object tracking. In *ICASSP 2022-2022 IEEE International Conference on Acoustics, Speech and Signal Processing (ICASSP)*, pages 2739–2743. IEEE, 2022.

[34] Yanpei Liu, Xinyun Chen, Chang Liu, and Dawn Song. Delving into transferable adversarial examples and black-box attacks. In *5th International Conference on Learning Representations, ICLR 2017, Toulon, France, April 24-26, 2017, Conference Track Proceedings*. OpenReview.net, 2017.

[35] Ze Liu, Yutong Lin, Yue Cao, Han Hu, Yixuan Wei, Zheng Zhang, Stephen Lin, and Baining Guo. Swin transformer: Hierarchical vision transformer using shifted windows. In *ICCV*, pages 9992–10002, 2021.

[36] Zihao Liu, Qi Liu, Tao Liu, Nuo Xu, Xue Lin, Yanzhi Wang, and Wujie Wen. Feature distillation: Dnn-oriented jpeg compression against adversarial examples. In *2019 IEEE/CVF Conference on Computer Vision and Pattern Recognition (CVPR)*, pages 860–868. IEEE, 2019.

[37] Yuyang Long, Qilong Zhang, Boheng Zeng, Lianli Gao, Xianglong Liu, Jian Zhang, and Jingkuan Song. Frequency domain model augmentation for adversarial attack. In *European Conference on Computer Vision*, 2022.

[38] Avery Ma, Amir-massoud Farahmand, Yangchen Pan, Philip Torr, and Jindong Gu. Improving adversarial transferability via model alignment. In *European Conference on Computer Vision*, pages 74–92. Springer, 2024.

[39] Aleksander Madry, Aleksandar Makelov, Ludwig Schmidt, Dimitris Tsipras, and Adrian Vladu. Towards deep learning models resistant to adversarial attacks. In *ICLR*, 2018.

[40] Sachin Mehta and Mohammad Rastegari. Mobilevit: Light-weight, general-purpose, and mobile-friendly vision transformer. In *The Tenth International Conference on Learning Representations, ICLR 2022, Virtual Event, April 25-29, 2022*, 2022.

[41] Muzammal Naseer, Salman H. Khan, Munawar Hayat, Fahad Shahbaz Khan, and Fatih Porikli. A self-supervised approach for adversarial robustness. In *2020 IEEE/CVF Conference on Computer Vision and Pattern Recognition, CVPR 2020, Seattle, WA, USA, June 13-19, 2020*, pages 259–268. Computer Vision Foundation / IEEE, 2020.

[42] Muzammal Naseer, Kanchana Ranasinghe, Salman Khan, Fahad Shahbaz Khan, and Fatih Porikli. On improving adversarial transferability of vision transformers. In *The Tenth International Conference on Learning Representations, ICLR 2022, Virtual Event, April 25-29, 2022*. OpenReview.net, 2022.

[43] Weili Nie, Brandon Guo, Yujia Huang, Chaowei Xiao, Arash Vahdat, and Anima Anandkumar. Diffusion models for adversarial purification. In *International Conference on Machine Learning (ICML)*, 2022.

[44] Zeyu Qin, Yanbo Fan, Yi Liu, Li Shen, Yong Zhang, Jue Wang, and Baoyuan Wu. Boosting the transferability of adversarial attacks with reverse adversarial perturbation. In *Advances in Neural Information Processing Systems 35: Annual Conference on Neural Information Processing Systems 2022, NeurIPS 2022, New Orleans, LA, USA, November 28 - December 9, 2022*, 2022.

[45] Ramprasaath R. Selvaraju, Michael Cogswell, Abhishek Das, Ramakrishna Vedantam, Devi Parikh, and Dhruv Batra. Grad-cam: Visual explanations from deep networks via gradient-based localization. *Int. J. Comput. Vis.*, 128(2):336–359, 2020.

[46] Karen Simonyan and Andrew Zisserman. Very deep convolutional networks for large-scale image recognition. In Yoshua Bengio and Yann LeCun, editors, *ICLR*, 2015.

[47] Zhimin Sun, Shen Chen, Taiping Yao, Ran Yi, Shouhong Ding, and Lizhuang Ma. Rethinking open-world deepfake attribution with multi-perspective sensory learning. *International Journal of Computer Vision*, 2024.

[48] Christian Szegedy, Vincent Vanhoucke, Sergey Ioffe, Jonathon Shlens, and Zbigniew Wojna. Rethinking the inception architecture for computer vision. In *2016 IEEE Conference on Computer Vision and Pattern Recognition, CVPR 2016, Las Vegas, NV, USA, June 27-30, 2016*, pages 2818–2826, 2016.

[49] Hugo Touvron, Matthieu Cord, Alexandre Sablayrolles, Gabriel Synnaeve, and Hervé Jégou. Going deeper with image transformers. In *2021 IEEE/CVF International Conference on Computer Vision, ICCV 2021, Montreal, QC, Canada, October 10-17, 2021*, pages 32–42. IEEE, 2021.

[50] Florian Tramèr, Alexey Kurakin, Nicolas Papernot, Ian J. Goodfellow, Dan Boneh, and Patrick D. McDaniel. Ensemble adversarial training: Attacks and defenses. In *International Conference on Learning Representations*, 2018.

[51] Jiafeng Wang, Zhaoyu Chen, Kaixun Jiang, Dingkang Yang, Lingyi Hong, Pinxue Guo, Haijing Guo, and Wenqiang Zhang. Boosting the transferability of adversarial attacks with global momentum initialization. *Expert Systems with Applications*, 255:124757, 2024.

[52] Wenhui Wang, Enze Xie, Xiang Li, Deng-Ping Fan, Kaitao Song, Ding Liang, Tong Lu, Ping Luo, and Ling Shao. PVT v2: Improved baselines with pyramid vision transformer. *Comput. Vis. Media*, 8(3):415–424, 2022.

[53] Xiaosen Wang and Kun He. Enhancing the transferability of adversarial attacks through variance tuning. In *IEEE Conference on Computer Vision and Pattern Recognition, CVPR 2021, virtual, June 19-25, 2021*, pages 1924–1933. Computer Vision Foundation / IEEE, 2021.

[54] Xiaosen Wang, Xuanran He, Jingdong Wang, and Kun He. Admix: Enhancing the transferability of adversarial attacks. In *Proceedings of the IEEE/CVF International Conference on Computer Vision*, pages 16158–16167, 2021.

[55] Xiaosen Wang, Kangheng Tong, and Kun He. Rethinking the backward propagation for adversarial transferability. In *Advances in Neural Information Processing Systems 36: Annual Conference on Neural Information Processing Systems 2023, NeurIPS 2023, New Orleans, LA, USA, December 10 - 16, 2023*, 2023.

[56] Xiaosen Wang, Zeliang Zhang, and Jianping Zhang. Structure invariant transformation for better adversarial transferability. In *Proceedings of the IEEE/CVF International Conference on Computer Vision (ICCV)*, pages 4607–4619, October 2023.

[57] Zeyu Wang, Xianhang Li, Hongru Zhu, and Cihang Xie. Revisiting adversarial training at scale. In *Proceedings of the IEEE/CVF Conference on Computer Vision and Pattern Recognition (CVPR)*, pages 24675–24685, June 2024.

[58] Zhipeng Wei, Jingjing Chen, Micah Goldblum, Zuxuan Wu, Tom Goldstein, and Yu-Gang Jiang. Towards transferable adversarial attacks on vision transformers. In *Thirty-Sixth AAAI Conference on Artificial Intelligence, AAAI 2022, Thirty-Fourth Conference on Innovative Applications of Artificial Intelligence, IAAI 2022, The Twelfth Symposium on Educational Advances in Artificial Intelligence, EAAI 2022 Virtual Event, February 22 - March 1, 2022*, pages 2668–2676. AAAI Press, 2022.

[59] Dongxian Wu, Yisen Wang, Shu-Tao Xia, James Bailey, and Xingjun Ma. Skip connections matter: On the transferability of adversarial examples generated with resnets. In *8th International Conference on Learning Representations, ICLR 2020, Addis Ababa, Ethiopia, April 26-30, 2020*. OpenReview.net, 2020.

[60] Cihang Xie, Jianyu Wang, Zhishuai Zhang, Zhou Ren, and Alan Yuille. Mitigating adversarial effects through randomization. *arXiv preprint arXiv:1711.01991*, 2017.

[61] Cihang Xie, Zhishuai Zhang, Yuyin Zhou, Song Bai, Jianyu Wang, Zhou Ren, and Alan L Yuille. Improving transferability of adversarial examples with input diversity. In *Proceedings of the IEEE/CVF Conference on Computer Vision and Pattern Recognition*, pages 2730–2739, 2019.

[62] Weilin Xu, David Evans, and Yanjun Qi. Feature squeezing: Detecting adversarial examples in deep neural networks. In *25th Annual Network and Distributed System Security Symposium, NDSS 2018, San Diego, California, USA, February 18-21, 2018*. The Internet Society, 2018.

[63] Dingkang Yang, Shuai Huang, Zhi Xu, Zhenpeng Li, Shunli Wang, Mingcheng Li, Yuzheng Wang, Yang Liu, Kun Yang, Zhaoyu Chen, et al. Aide: A vision-driven multi-view, multi-modal, multi-tasking dataset for assistive driving perception. In *Proceedings of the IEEE/CVF International Conference on Computer Vision*, pages 20459–20470, 2023.

[64] Xiao Yang, Yinpeng Dong, Tianyu Pang, Hang Su, and Jun Zhu. Boosting transferability of targeted adversarial examples via hierarchical generative networks. In *Computer Vision - ECCV 2022 - 17th European Conference, Tel Aviv, Israel, October 23-27, 2022, Proceedings, Part IV*, volume 13664 of *Lecture Notes in Computer Science*, pages 725–742. Springer, 2022.

[65] Hongyi Zhang, Moustapha Cissé, Yann N. Dauphin, and David Lopez-Paz. mixup: Beyond empirical risk minimization. In *6th International Conference on Learning Representations, ICLR 2018, Vancouver, BC, Canada, April 30 - May 3, 2018, Conference Track Proceedings*. OpenReview.net, 2018.

[66] Jianping Zhang, Yizhan Huang, Weibin Wu, and Michael R. Lyu. Transferable adversarial attacks on vision transformers with token gradient regularization. In *IEEE/CVF Conference on Computer Vision and Pattern Recognition, CVPR 2023, Vancouver, BC, Canada, June 17-24, 2023*, pages 16415–16424. IEEE, 2023.

[67] Jingyu Zhang, Kun Yang, Hanqi Wang, Peng Sun, and Liang Song. Efficient vehicular collaborative perception based on saptial-temporal feature compression. *IEEE Transactions on Vehicular Technology*, 2024.

[68] Jingyu Zhang, Kun Yang, Yilei Wang, Hanqi Wang, Peng Sun, and Liang Song. Ermvp: Communication-efficient and collaboration-robust multi-vehicle perception in challenging environments. In *Proceedings of the IEEE/CVF Conference on Computer Vision and Pattern Recognition (CVPR)*, pages 12575–12584, June 2024.

[69] Tianyi Zheng, Bo Li, Shuang Wu, Ben Wan, Guodong Mu, Shice Liu, Shouhong Ding, and Jia Wang. MFAE: masked frequency autoencoders for domain generalization face anti-spoofing. *IEEE Trans. Inf. Forensics Secur.*, 19:4058–4069, 2024.

- [70] Tianyi Zheng, Qinji Yu, Zhaoyu Chen, and Jia Wang. Famim: A novel frequency-domain augmentation masked image model framework for domain generalizable face anti-spoofing. In *ICASSP 2024 - 2024 IEEE International Conference on Acoustics, Speech and Signal Processing (ICASSP)*, pages 4470–4474, 2024.
- [71] Daquan Zhou, Zhiding Yu, Enze Xie, Chaowei Xiao, Animashree Anandkumar, Jiashi Feng, and Jose M Alvarez. Understanding the robustness in vision transformers. In *International conference on machine learning*, pages 27378–27394. PMLR, 2022.
- [72] Xinyu Zhou, Pinxue Guo, Lingyi Hong, Jinglun Li, Wei Zhang, Weifeng Ge, and Wenqiang Zhang. Reading relevant feature from global representation memory for visual object tracking. In *Advances in Neural Information Processing Systems*, volume 36, pages 10814–10827, 2023.

This document provides more details of Spatial Adversarial Alignment (SAA), organized as follows:

- In Section A, we describe related work to this paper, including transfer attacks on CNNs and ViT.
- In Section B, we describe the detail loss calculation, corresponding to Section 2.2 of the main body.
- In Section C, we supplement the more ablation studies, corresponding to Section 2.4.3 of the main body.
- In Section D, we supplement feature-based transfer attacks with SAA, corresponding to Section 2.4 of the main body.
- In Section E, we present additional Grad-CAM visualizations on target models to analyze the impact of SAA.
- We provide the implementation of our Spatial Adversarial Alignment (SAA) in the **Core Codes of Supplementary Material**.

## A Related Work

### A.1 Transfer attacks on CNNs

Early transfer attacks are mainly conducted between CNNs, and the most popular methods were advanced optimization [13, 29, 51], data augmentation [61, 14, 37], and model modification [59, 21, 58].

**Advanced Optimization.** [29] compare adversarial attacks to model training: better optimization methods can obtain models with better generalization, and therefore also generate adversarial examples with higher transferability. FGSM [18] is the earliest gradient-based transfer attack, which was then extended to I-FGSM [27]. The subsequent advance optimization further improves the transferability by introducing momentum [13, 29, 53, 51] and smoothness [44].

**Data Augmentation.** Data augmentation serves as an effective strategy to prevent model overfitting, achieving state-of-the-art performance in model generalization [65, 12]. Building on this principle, numerous adversarial attacks incorporate various transformations to enhance adversarial transferability, including modifications in size [61], scale [29], mixup [54], and frequency domain [37] adjustments. This integration aims to mitigate the overfitting of adversarial examples to the surrogate model, thereby increasing their effectiveness across different models.

**Model Modification.** According to certain characteristics of the model, modifying the parameters of the surrogate model or changing the forward or backward propagation can also improve the transferability. Skip Gradient Method (SGM) [59] using more gradients from the skip connections rather than the residual modules, allows one to craft adversarial examples with high transferability. Similarly, Linear Backpropagation (LinBP) [21] and Backward Propagation Attack (BPA) [55] concentrate on non-linear activations by modifying the ReLU derivatives to enhance attack transferability. Model Alignment (MA) [38] promotes alignment of model predictions through an alignment loss relative to a witness model, with the aim of capturing shared features across models. However, MA overlooks spatial and adversarial feature alignment across architectures, limiting its effectiveness. Unlike these methods, our SAA requires no modifications to the forward or backpropagation processes, enabling the efficient generation of highly transferable adversarial examples with minimal training overhead. In contrast, LinBP and BPA, involve altering backpropagation or even full model retraining, incurring significantly higher computational costs.

### A.2 Transfer attacks on ViTs

Current transfer attacks for ViTs largely adapt methods developed for CNNs. Pay No Attention (PNA) [58] method extends Skip Gradient Method (SGM) to ViTs by omitting the gradient computation of attention blocks during back-propagation, thereby enhancing adversarial transferability. PatchOut [58] strategy selects a random subset of image patches to compute the gradient at each iteration, functioning as an image transformation technique to increase transferability. Then, Self-Ensemble (SE) [42] approach employs the class token at each layer with a shared classification

head to create an ensemble model, facilitating optimized perturbation; however, many ViTs, such as Visformer [8] and CaiT [49], lack sufficient class tokens to build this ensemble. Additionally, Token Refinement (TR) [42] module fine-tunes class tokens to further boost transferability. Recently, Token Gradient Regularization (TGR) [66] works from the perspective of variance reduction, stabilizing the gradient direction to prevent adversarial examples from getting stuck in poor local optima. Distinct from these approaches, SAA is the first method to specifically analyze architectural differences across models. By leveraging shared features between different architectures, SAA enables the creation of more generalized surrogate models that integrate seamlessly with optimization and data augmentation methods, ultimately achieving state-of-the-art transferability.

---

**Algorithm 1** Loss  $\mathcal{L}_{SAA}$ 


---

**Require:** Input  $x$ , surrogate model  $f_{\theta_s}$ , witness model  $f_{\theta_w}$   
**Ensure:**  $\mathcal{L}_{SAA}$

- 1: **#Preliminaries**
- 2: **if**  $f_{\theta}$  is CNN **then**
- 3:     Compute global logits:  

$$f_{\theta}(x) = \text{Classifier}(\text{GlobalAvgPooling}(\text{Backbone}(x)))$$
- 4:     Obtain local regions collection  $z$ :  

$$z_{\theta}(x) = \text{Classifier}(\text{Backbone}(x))$$
- 5: **else if**  $f$  is ViT **then**
- 6:      $z' = \text{TransformerEncoder}(x)$
- 7:     Compute global logits:  

$$f_{\theta}(x) = \text{Classifier}(z'[0])$$
- 8:     Obtain local regions collection  $z$ :  

$$z_{\theta}(x) = \text{Classifier}(z'[1 :])$$
- 9: **end if**
- 10: **#Step 1: Compute spatial-aware alignment loss**
- 11: Obtain global logits  $f_{\theta_s}(x)$  and  $f_{\theta_w}(x)$
- 12: Compute  $\mathcal{L}_{global}(x; \theta_s) = D_{KL}(f_{\theta_s}(x), f_{\theta_w}(x))$
- 13: **for** each local region  $q$  **do**
- 14:     Obtain local logits  $z_{\theta_s}^{[q]}$  and  $z_{\theta_w}^{[q]}$
- 15:     Derive pseudo-label  $\hat{y}_{\theta_w}^{[q]} = \arg \max(z_{\theta_w}^{[q]}(x))$
- 16:     Compute local alignment loss for region  $q$ :  $D_{CE}(z_{\theta_s}^{[q]}(x), \hat{y}_{\theta_w}^{[q]})$
- 17: **end for**
- 18: Calculate total local alignment loss:  $\mathcal{L}_{local}(x; \theta_s) = \frac{1}{HW} \sum_{q=1}^{HW} D_{CE}(z_{\theta_s}^{[q]}(x), \arg \max(z_{\theta_w}^{[q]}(x)))$
- 19: Calculate spatial-aware alignment loss:  $\mathcal{L}_{SA}(x; \theta_s) = \mathcal{L}_{global}(x; \theta_s) + \gamma \cdot \mathcal{L}_{local}(x; \theta_s)$
- 20: **#Step 2: Compute adversarial-aware alignment loss**
- 21: Initialize adversarial example  $x_{\text{adv}}^{(0)} = x$
- 22: **for** each iteration  $t$  **do**
- 23:      $x_{\text{adv}}^{(t+1)} = \Pi_{x, \epsilon} \left( x_{\text{adv}}^{(t)} + \alpha \cdot \text{sign} \left( \nabla_x D_{KL} \left( f_{\theta_s}(x_{\text{adv}}^{(t)}), f_{\theta_w}(x) \right) \right) \right)$
- 24: **end for**
- 25: Obtain final adversarial example  $x_{\text{adv}} = x_{\text{adv}}^{(T)}$
- 26: Calculate adversarial-aware alignment loss:  $\mathcal{L}_{AA}(x_{\text{adv}}; \theta_s) = \mathcal{L}_{global}(x_{\text{adv}}; \theta_s) + \omega \cdot \mathcal{L}_{local}(x_{\text{adv}}; \theta_s)$
- 27: **#Step 3: Calculate spatial adversarial alignment loss**
- 28:  $\mathcal{L}_{SAA}(x; \theta_s) = \mathcal{L}_{SA}(x; \theta_s) + \kappa \cdot \mathcal{L}_{AA}(x_{\text{adv}}; \theta_s)$
- 29: **Return**  $\mathcal{L}_{SAA}$

---

## B Loss Calculation

We introduce the calculation of loss in detail, as shown in Algorithm 1. For the specific implementation, please refer to the code provided in **Supplementary Material**.

Table 8: Ablation study on distance metrics of global features.

Loss	Target Model										Avg. ASR (%)	
	CNNs						ViTs					
	Res18	Res50	Res101	VGG19	DN121	Inc-v3	ViT-B	Swin-B	PVT-v2	MobViT		
n/a	57.7	99.9	58.1	54.2	55.1	39.0	9.4	33.0	38.0	35.7	42.2	
KL	84.1	99.6	74.7	80.3	81.8	65.7	24.3	48.7	52.9	62.5	63.9	
TV	62.1	97.8	56.2	67.5	63.9	47.6	9.4	32.2	37.2	44.1	46.7	
JS	83.3	99.1	70.0	78.2	80.9	63.5	22.8	46.4	49.3	58.5	61.4	
NCE	78.8	99.3	69.1	77.0	76.6	60.3	21.7	46.2	48.2	55.8	59.3	

Table 9: Ablation study on different supervision in self-adversarial strategy.

Source	Witness	Attack	Res18	Res50	Res101	VGG19	DN121	IncV3	ViT-B	Swin-B	PVT-v2	MobViT	Avg. ASR (%)
			MA	74.2	99.2	63.5	69.3	72.8	51.5	18.5	41.5	42.7	53.5
Res50	ViT-B	SAA ( $f_{\theta_w}(x)$ )	84.1	99.6	74.7	80.3	81.8	65.7	24.3	48.7	52.9	62.5	63.9
		SAA ( $f_{\theta_s}(x)$ )	81.1	96.6	68.7	77.5	79.5	60.6	19.4	45.9	46.2	57.6	59.6

## C Ablation Study

We select ResNet, DenseNet, and Swin, all of which have won Best Paper Awards, and ViT, which is a pioneering work. These models are representative of both CNNs and ViTs and their weights are all from *timm*, ensuring the generalization of our conclusions. We conduct 16 combinations of experiments and evaluate on 6 CNNs and 4 ViTs, showing that SAA’s improvement is not limited to specific choices of witness models.

**Training Epochs.** In Section 3.2, we reveal the powerful potential of SAA for adversarial transferability after training for only one epoch. Furthermore, we explore the performance difference after training for multiple epochs, as shown in Figure 3. We calculate the average attack success rate except for the Res50 surrogate model itself and find that with the increase of epochs, the adversarial transferability of the aligned surrogate model is further improved, reaching convergence around the 9-th epoch. Compared with MA, SAA can achieve higher transferability in small epochs, and after multiple rounds of training, the transferability has a higher upper limit, which shows the importance of using spatial and adversarial features for model alignment.

**Distance Metric.** There are many ways to align the output of global features. To better align the global features, we select Kullback–Leibler Divergence (KL), Total Variation (TV), Jensen–Shannon Divergence (JS), and NCE [2] loss for evaluation. We select ResNet-50 as the surrogate model and ViT-B as the witness model for ablation studies. As shown in Table 8, KL exceeds the next best JS by 2.5%, so we choose KL as the metric.

**GPU Memory and Computing Cost.** SAA’s GPU memory is split into alignment and attack. In alignment, we infer the witness model and train the surrogate model for one epoch, so the memory usage is the sum of both. When the surrogate is Res50 and the witness is ViT-B, SAA’s GPU memory is only 2794MB with a batch size of 1. Once alignment is complete, attack costs only are an aligned surrogate model, making SAA’s memory the same as SOTA attacks without extra memory. Thus, its GPU memory is acceptable. For computing cost, SAA needs about 10 hours’ training time on ImageNet with batch size of 64 under Nvidia RTX 3090. The total computational cost of MA is 2 hours with the same setting. Since adversarial-aware alignment introduces the solution of adversarial examples, in the practice of SAA, model training takes about 2 hours, and solving adversarial examples takes about 8 hours, for a total of 10 hours. Note that the main computational bottleneck is actually obtaining adversarial examples, not model training. Some newer adversarial

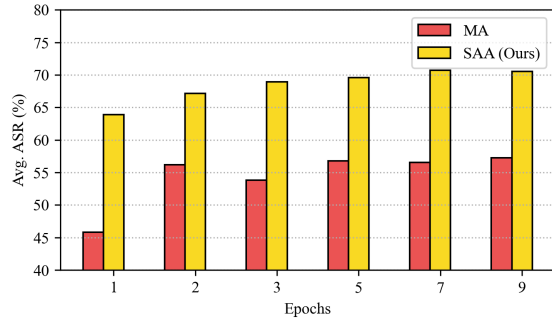


Figure 3: Ablation study on training epochs.

Table 10: Ablation study on label supervision in local alignment.

Source	Witness	Attack	Res18	Res50	Res101	VGG19	DN121	IncV3	ViT-B	Swin-B	PVT_v2	MobViT	Avg.	ASR (%)
Res50	ViT-B	SAA-MI (Ours)	<b>84.1</b>	<b>99.6</b>	<b>74.7</b>	<b>80.3</b>	<b>81.8</b>	<b>65.7</b>	<b>24.3</b>	<b>48.7</b>	<b>52.9</b>	<b>62.5</b>	<b>63.9</b>	
		SAA-MI (soft)	81.9	96.4	65.9	74.5	77.7	60.8	18.8	44.4	43.1	53.0	57.8	

Table 11: SAA improves the adversarial transferability of feature-based transfer attacks.

Attack	Target Model										Avg. ASR (%)	
	CNNs					ViTs						
	Res18	Res50	Res101	VGG19	DN121	Inc-v3	ViT-B	Swin-B	PVT-v2	MobViT		
FDA	55.2	31.6	36.8	52.0	43.6	27.1	2.7	21.0	24.5	27.8	32.3	
FDA-SAA	<b>82.9</b>	<b>79.0</b>	<b>72.5</b>	<b>79.1</b>	<b>77.1</b>	<b>60.1</b>	<b>14.4</b>	<b>39.5</b>	<b>43.4</b>	<b>58.4</b>	<b>58.6</b>	
FDA-MI	75.0	46.1	60.6	74.0	65.3	46.0	8.4	27.3	29.4	47.0	48.1	
FDA-MI-SAA	<b>89.7</b>	<b>88.2</b>	<b>81.7</b>	<b>86.9</b>	<b>85.3</b>	<b>73.1</b>	<b>21.9</b>	<b>41.7</b>	<b>44.7</b>	<b>68.9</b>	<b>66.0</b>	

attack techniques [57] may be able to accelerate this process and reduce the time to 1/3 of the original, which is an auspicious research direction.

**Different supervision in self-adversarial strategy.** In SAA, adversarial-aware alignment is performed using the self-adversarial strategy, where the supervision comes from global features of the witness model. Here, we investigate whether supervision from global features of the surrogate model or global features of the witness model is more effective, and compare both approaches with the MA [38] baseline. The results in Table 9 show that SAA ( $f_{\theta_w}(x)$ ) outperforms SAA ( $f_{\theta_s}(x)$ ) by 4.3% in ASR, indicating that  $f_{\theta_w}(x)$  provides stronger supervision for adversarial-aware alignment, leading to highly transferable adversarial examples. This highlights the effectiveness of alignment using  $f_{\theta_w}(x)$  and its superiority over  $f_{\theta_s}(x)$ , demonstrating that leveraging witness model features enhances adversarial robustness.

**Label supervision in local alignment.** We add experiments using soft labels (logits) and the KL divergence loss function for local alignment, as shown in Table 10. The surrogate model is Res50 and the witness model is ViT-B. In this scenario, using hard labels (local pseudo-labels) achieves higher adversarial transferability (improving ASR by 6.1%).

## D Feature-based Transfer Attacks

Here we combine SAA with feature-based transfer attacks for experiments, as shown in Table 11. Here we select ResNet-50 as the surrogate model and ViT-B as the witness model. Since the aligned surrogate model after SAA can learn more common features, SAA further improves the attack performance of FDA [17]. On FDA and FDA-MI, SAA improves the black-box attack success rate by 25.7% and 17.1%, respectively.

## E Grad-CAM Visualization

We present Grad-CAM visualizations on two target models: ResNet-101 and ViT-S, as shown in Figure 4. Each set consists of three columns: the first column shows the Grad-CAM heatmap of the target model on clean input; the second column displays the heatmap for adversarial examples generated by the unaligned model; the third column corresponds to adversarial examples generated by SAA aligned model. The visualizations indicate that adversarial examples from the unaligned model produce heatmap distributions more similar to those of clean inputs, whereas adversarial examples from the aligned model effectively disrupt the target model’s attention distribution, leading to a more thorough attack.

## F Security Implications

**Potential misuse.** SAA improves the cross-architecture adversarial transferability of surrogate models, which means attacks against unknown systems pose a higher threat. For example, for a face forgery detection system [3], open-source models are typically CNNs, while the most advanced

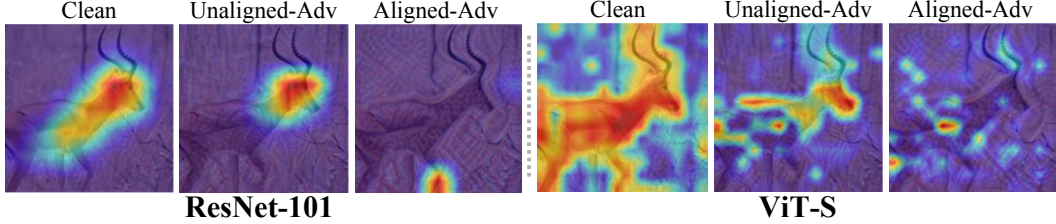


Figure 4: Grad-CAM on target models.

commercial applications may already be ViT-based models. In this case, using existing CNN detectors as surrogate models, combined with SAA, can lead to successful attack on commercial applications.

**Mitigation strategies.** We think that potential defense strategies primarily involve introducing adversarial training and increasing model diversity. The former recommends introducing a small number of adversarial examples during model training to improve robustness against adversarial examples. The latter recommends introducing multi-model ensemble training during training to increase the model’s feature complexity and enhance deployment robustness.

## NeurIPS Paper Checklist

### 1. Claims

Question: Do the main claims made in the abstract and introduction accurately reflect the paper's contributions and scope?

Answer: [\[Yes\]](#)

Justification: The abstract and introduction has accurately reflected the paper's contributions and scope.

Guidelines:

- The answer NA means that the abstract and introduction do not include the claims made in the paper.
- The abstract and/or introduction should clearly state the claims made, including the contributions made in the paper and important assumptions and limitations. A No or NA answer to this question will not be perceived well by the reviewers.
- The claims made should match theoretical and experimental results, and reflect how much the results can be expected to generalize to other settings.
- It is fine to include aspirational goals as motivation as long as it is clear that these goals are not attained by the paper.

### 2. Limitations

Question: Does the paper discuss the limitations of the work performed by the authors?

Answer: [\[Yes\]](#)

Justification: This paper has discussed the limitiations of this work.

Guidelines:

- The answer NA means that the paper has no limitation while the answer No means that the paper has limitations, but those are not discussed in the paper.
- The authors are encouraged to create a separate "Limitations" section in their paper.
- The paper should point out any strong assumptions and how robust the results are to violations of these assumptions (e.g., independence assumptions, noiseless settings, model well-specification, asymptotic approximations only holding locally). The authors should reflect on how these assumptions might be violated in practice and what the implications would be.
- The authors should reflect on the scope of the claims made, e.g., if the approach was only tested on a few datasets or with a few runs. In general, empirical results often depend on implicit assumptions, which should be articulated.
- The authors should reflect on the factors that influence the performance of the approach. For example, a facial recognition algorithm may perform poorly when image resolution is low or images are taken in low lighting. Or a speech-to-text system might not be used reliably to provide closed captions for online lectures because it fails to handle technical jargon.
- The authors should discuss the computational efficiency of the proposed algorithms and how they scale with dataset size.
- If applicable, the authors should discuss possible limitations of their approach to address problems of privacy and fairness.
- While the authors might fear that complete honesty about limitations might be used by reviewers as grounds for rejection, a worse outcome might be that reviewers discover limitations that aren't acknowledged in the paper. The authors should use their best judgment and recognize that individual actions in favor of transparency play an important role in developing norms that preserve the integrity of the community. Reviewers will be specifically instructed to not penalize honesty concerning limitations.

### 3. Theory assumptions and proofs

Question: For each theoretical result, does the paper provide the full set of assumptions and a complete (and correct) proof?

Answer: [\[NA\]](#)

Justification: This paper doesn't provide the theoretical analysis.

Guidelines:

- The answer NA means that the paper does not include theoretical results.
- All the theorems, formulas, and proofs in the paper should be numbered and cross-referenced.
- All assumptions should be clearly stated or referenced in the statement of any theorems.
- The proofs can either appear in the main paper or the supplemental material, but if they appear in the supplemental material, the authors are encouraged to provide a short proof sketch to provide intuition.
- Inversely, any informal proof provided in the core of the paper should be complemented by formal proofs provided in appendix or supplemental material.
- Theorems and Lemmas that the proof relies upon should be properly referenced.

#### 4. Experimental result reproducibility

Question: Does the paper fully disclose all the information needed to reproduce the main experimental results of the paper to the extent that it affects the main claims and/or conclusions of the paper (regardless of whether the code and data are provided or not)?

Answer: **[Yes]**

Justification: We provide the detailed parameters and release the codes to reproduce the main experimental results.

Guidelines:

- The answer NA means that the paper does not include experiments.
- If the paper includes experiments, a No answer to this question will not be perceived well by the reviewers: Making the paper reproducible is important, regardless of whether the code and data are provided or not.
- If the contribution is a dataset and/or model, the authors should describe the steps taken to make their results reproducible or verifiable.
- Depending on the contribution, reproducibility can be accomplished in various ways. For example, if the contribution is a novel architecture, describing the architecture fully might suffice, or if the contribution is a specific model and empirical evaluation, it may be necessary to either make it possible for others to replicate the model with the same dataset, or provide access to the model. In general, releasing code and data is often one good way to accomplish this, but reproducibility can also be provided via detailed instructions for how to replicate the results, access to a hosted model (e.g., in the case of a large language model), releasing of a model checkpoint, or other means that are appropriate to the research performed.
- While NeurIPS does not require releasing code, the conference does require all submissions to provide some reasonable avenue for reproducibility, which may depend on the nature of the contribution. For example
  - (a) If the contribution is primarily a new algorithm, the paper should make it clear how to reproduce that algorithm.
  - (b) If the contribution is primarily a new model architecture, the paper should describe the architecture clearly and fully.
  - (c) If the contribution is a new model (e.g., a large language model), then there should either be a way to access this model for reproducing the results or a way to reproduce the model (e.g., with an open-source dataset or instructions for how to construct the dataset).
  - (d) We recognize that reproducibility may be tricky in some cases, in which case authors are welcome to describe the particular way they provide for reproducibility. In the case of closed-source models, it may be that access to the model is limited in some way (e.g., to registered users), but it should be possible for other researchers to have some path to reproducing or verifying the results.

#### 5. Open access to data and code

Question: Does the paper provide open access to the data and code, with sufficient instructions to faithfully reproduce the main experimental results, as described in supplemental material?

Answer: [\[Yes\]](#)

Justification: The data is publicly available and we release the codes to reproduce the main experimental results.

Guidelines:

- The answer NA means that paper does not include experiments requiring code.
- Please see the NeurIPS code and data submission guidelines (<https://nips.cc/public/guides/CodeSubmissionPolicy>) for more details.
- While we encourage the release of code and data, we understand that this might not be possible, so “No” is an acceptable answer. Papers cannot be rejected simply for not including code, unless this is central to the contribution (e.g., for a new open-source benchmark).
- The instructions should contain the exact command and environment needed to run to reproduce the results. See the NeurIPS code and data submission guidelines (<https://nips.cc/public/guides/CodeSubmissionPolicy>) for more details.
- The authors should provide instructions on data access and preparation, including how to access the raw data, preprocessed data, intermediate data, and generated data, etc.
- The authors should provide scripts to reproduce all experimental results for the new proposed method and baselines. If only a subset of experiments are reproducible, they should state which ones are omitted from the script and why.
- At submission time, to preserve anonymity, the authors should release anonymized versions (if applicable).
- Providing as much information as possible in supplemental material (appended to the paper) is recommended, but including URLs to data and code is permitted.

## 6. Experimental setting/details

Question: Does the paper specify all the training and test details (e.g., data splits, hyper-parameters, how they were chosen, type of optimizer, etc.) necessary to understand the results?

Answer: [\[Yes\]](#)

Justification: We provide the detailed parameters and release the codes to reproduce the main experimental results.

Guidelines:

- The answer NA means that the paper does not include experiments.
- The experimental setting should be presented in the core of the paper to a level of detail that is necessary to appreciate the results and make sense of them.
- The full details can be provided either with the code, in appendix, or as supplemental material.

## 7. Experiment statistical significance

Question: Does the paper report error bars suitably and correctly defined or other appropriate information about the statistical significance of the experiments?

Answer: [\[NA\]](#)

Justification: Because of the huge computing cost.

Guidelines:

- The answer NA means that the paper does not include experiments.
- The authors should answer “Yes” if the results are accompanied by error bars, confidence intervals, or statistical significance tests, at least for the experiments that support the main claims of the paper.
- The factors of variability that the error bars are capturing should be clearly stated (for example, train/test split, initialization, random drawing of some parameter, or overall run with given experimental conditions).
- The method for calculating the error bars should be explained (closed form formula, call to a library function, bootstrap, etc.)
- The assumptions made should be given (e.g., Normally distributed errors).

- It should be clear whether the error bar is the standard deviation or the standard error of the mean.
- It is OK to report 1-sigma error bars, but one should state it. The authors should preferably report a 2-sigma error bar than state that they have a 96% CI, if the hypothesis of Normality of errors is not verified.
- For asymmetric distributions, the authors should be careful not to show in tables or figures symmetric error bars that would yield results that are out of range (e.g. negative error rates).
- If error bars are reported in tables or plots, The authors should explain in the text how they were calculated and reference the corresponding figures or tables in the text.

## 8. Experiments compute resources

Question: For each experiment, does the paper provide sufficient information on the computer resources (type of compute workers, memory, time of execution) needed to reproduce the experiments?

Answer: [\[Yes\]](#)

Justification: We describe the the computer resources in Appendix.

Guidelines:

- The answer NA means that the paper does not include experiments.
- The paper should indicate the type of compute workers CPU or GPU, internal cluster, or cloud provider, including relevant memory and storage.
- The paper should provide the amount of compute required for each of the individual experimental runs as well as estimate the total compute.
- The paper should disclose whether the full research project required more compute than the experiments reported in the paper (e.g., preliminary or failed experiments that didn't make it into the paper).

## 9. Code of ethics

Question: Does the research conducted in the paper conform, in every respect, with the NeurIPS Code of Ethics <https://neurips.cc/public/EthicsGuidelines>?

Answer: [\[Yes\]](#)

Justification: Everything preserves anonymity.

Guidelines:

- The answer NA means that the authors have not reviewed the NeurIPS Code of Ethics.
- If the authors answer No, they should explain the special circumstances that require a deviation from the Code of Ethics.
- The authors should make sure to preserve anonymity (e.g., if there is a special consideration due to laws or regulations in their jurisdiction).

## 10. Broader impacts

Question: Does the paper discuss both potential positive societal impacts and negative societal impacts of the work performed?

Answer: [\[Yes\]](#)

Justification: We discuss this in last section.

Guidelines:

- The answer NA means that there is no societal impact of the work performed.
- If the authors answer NA or No, they should explain why their work has no societal impact or why the paper does not address societal impact.
- Examples of negative societal impacts include potential malicious or unintended uses (e.g., disinformation, generating fake profiles, surveillance), fairness considerations (e.g., deployment of technologies that could make decisions that unfairly impact specific groups), privacy considerations, and security considerations.

- The conference expects that many papers will be foundational research and not tied to particular applications, let alone deployments. However, if there is a direct path to any negative applications, the authors should point it out. For example, it is legitimate to point out that an improvement in the quality of generative models could be used to generate deepfakes for disinformation. On the other hand, it is not needed to point out that a generic algorithm for optimizing neural networks could enable people to train models that generate Deepfakes faster.
- The authors should consider possible harms that could arise when the technology is being used as intended and functioning correctly, harms that could arise when the technology is being used as intended but gives incorrect results, and harms following from (intentional or unintentional) misuse of the technology.
- If there are negative societal impacts, the authors could also discuss possible mitigation strategies (e.g., gated release of models, providing defenses in addition to attacks, mechanisms for monitoring misuse, mechanisms to monitor how a system learns from feedback over time, improving the efficiency and accessibility of ML).

## 11. Safeguards

Question: Does the paper describe safeguards that have been put in place for responsible release of data or models that have a high risk for misuse (e.g., pretrained language models, image generators, or scraped datasets)?

Answer: [NA]

Justification: the paper poses no such risks.

Guidelines:

- The answer NA means that the paper poses no such risks.
- Released models that have a high risk for misuse or dual-use should be released with necessary safeguards to allow for controlled use of the model, for example by requiring that users adhere to usage guidelines or restrictions to access the model or implementing safety filters.
- Datasets that have been scraped from the Internet could pose safety risks. The authors should describe how they avoided releasing unsafe images.
- We recognize that providing effective safeguards is challenging, and many papers do not require this, but we encourage authors to take this into account and make a best faith effort.

## 12. Licenses for existing assets

Question: Are the creators or original owners of assets (e.g., code, data, models), used in the paper, properly credited and are the license and terms of use explicitly mentioned and properly respected?

Answer: [Yes]

Justification: We have cited the original paper that produced the code package or dataset.

Guidelines:

- The answer NA means that the paper does not use existing assets.
- The authors should cite the original paper that produced the code package or dataset.
- The authors should state which version of the asset is used and, if possible, include a URL.
- The name of the license (e.g., CC-BY 4.0) should be included for each asset.
- For scraped data from a particular source (e.g., website), the copyright and terms of service of that source should be provided.
- If assets are released, the license, copyright information, and terms of use in the package should be provided. For popular datasets, [paperswithcode.com/datasets](https://paperswithcode.com/datasets) has curated licenses for some datasets. Their licensing guide can help determine the license of a dataset.
- For existing datasets that are re-packaged, both the original license and the license of the derived asset (if it has changed) should be provided.

- If this information is not available online, the authors are encouraged to reach out to the asset's creators.

### 13. New assets

Question: Are new assets introduced in the paper well documented and is the documentation provided alongside the assets?

Answer: [NA]

Justification: This paper does not release new assets.

Guidelines:

- The answer NA means that the paper does not release new assets.
- Researchers should communicate the details of the dataset/code/model as part of their submissions via structured templates. This includes details about training, license, limitations, etc.
- The paper should discuss whether and how consent was obtained from people whose asset is used.
- At submission time, remember to anonymize your assets (if applicable). You can either create an anonymized URL or include an anonymized zip file.

### 14. Crowdsourcing and research with human subjects

Question: For crowdsourcing experiments and research with human subjects, does the paper include the full text of instructions given to participants and screenshots, if applicable, as well as details about compensation (if any)?

Answer: [NA]

Justification: This paper does not involve crowdsourcing nor research with human subjects.

Guidelines:

- The answer NA means that the paper does not involve crowdsourcing nor research with human subjects.
- Including this information in the supplemental material is fine, but if the main contribution of the paper involves human subjects, then as much detail as possible should be included in the main paper.
- According to the NeurIPS Code of Ethics, workers involved in data collection, curation, or other labor should be paid at least the minimum wage in the country of the data collector.

### 15. Institutional review board (IRB) approvals or equivalent for research with human subjects

Question: Does the paper describe potential risks incurred by study participants, whether such risks were disclosed to the subjects, and whether Institutional Review Board (IRB) approvals (or an equivalent approval/review based on the requirements of your country or institution) were obtained?

Answer: [NA]

Justification: This paper does not involve crowdsourcing nor research with human subjects.

Guidelines:

- The answer NA means that the paper does not involve crowdsourcing nor research with human subjects.
- Depending on the country in which research is conducted, IRB approval (or equivalent) may be required for any human subjects research. If you obtained IRB approval, you should clearly state this in the paper.
- We recognize that the procedures for this may vary significantly between institutions and locations, and we expect authors to adhere to the NeurIPS Code of Ethics and the guidelines for their institution.
- For initial submissions, do not include any information that would break anonymity (if applicable), such as the institution conducting the review.

### 16. Declaration of LLM usage

Question: Does the paper describe the usage of LLMs if it is an important, original, or non-standard component of the core methods in this research? Note that if the LLM is used only for writing, editing, or formatting purposes and does not impact the core methodology, scientific rigorosity, or originality of the research, declaration is not required.

Answer: [NA]

Justification: The core method development in this research does not involve LLMs as any important, original, or non-standard components.

Guidelines:

- The answer NA means that the core method development in this research does not involve LLMs as any important, original, or non-standard components.
- Please refer to our LLM policy (<https://neurips.cc/Conferences/2025/LLM>) for what should or should not be described.